4-27-2010

Bifurcations of traveling wave solutions for an integrable equation

Jibin Li
Zhejiang Normal University

Zhijun Qiao
The University of Texas Rio Grande Valley, zhijun.qiao@utrgv.edu

JOURNAL OF MATHEMATICAL PHYSICS **51**, 042703 (2010)

Bifurcations of traveling wave solutions for an integrable equation

Jibin Li[1,a)] and Zhijun Qiao[2,b)]
[1]*Department of Mathematics, Zhejiang Normal University, Jinhua, Zhejiang 321004, People's Republic of China and Kunming University of Science and Technology, Kunming, Yunnan 650093, People's Republic of China*
[2]*Department of Mathematics, The University of Texas Pan-American, 1201 West University Drive, Edinburg, Texas 78541, USA*

(Received 14 December 2009; accepted 12 March 2010; published online 27 April 2010)

This paper deals with the following equation $m_t=(1/2)(1/m^k)_{xxx}-(1/2)(1/m^k)_x$, which is proposed by Z. J. Qiao [J. Math. Phys. **48**, 082701 (2007)] and Qiao and Liu [Chaos, Solitons Fractals **41**, 587 (2009)]. By adopting the phase analysis method of planar dynamical systems and the theory of the singular traveling wave systems to the traveling wave solutions of the equation, it is shown that for different k, the equation may have infinitely many solitary wave solutions, periodic wave solutions, kink/antikink wave solutions, cusped solitary wave solutions, and breaking loop solutions. We discuss in a detail the cases of $k=-2,-\frac{1}{2},\frac{1}{2},2$, and parametric representations of all possible bounded traveling wave solutions are given in the different (c,g)-parameter regions. © *2010 American Institute of Physics.*
[doi:10.1063/1.3385777]

I. INTRODUCTION

The investigation of the traveling wave solutions to nonlinear evolution equations plays an important role in the mathematical physics. For example, the wave phenomena observed in fluid dynamics, plasma, and elastic media are often modeled by the bell shaped or kink shaped traveling wave solutions. Since 1970s, much significant progress has been made in the development of theory and approach, such as inverse scattering transformation method,[1] Darboux and Bäcklund transformation,[2–4] Hirota bilinear method,[5] phase analysis method,[6,7] and so on. In this paper, we study the following equation proposed in Refs. 8 and 9:

$$m_t=\frac{1}{2}\left(\frac{1}{m^k}\right)_{xxx}-\frac{1}{2}\left(\frac{1}{m^k}\right)_x, \tag{1}$$

where $k\in\mathbf{R}$, $k\neq -1,0$. Apparently, when $k=\frac{1}{2}$, (1) reads as a Harry Dym-type equation, which is actually the first member in the positive Camassa–Holm hierarchy.[10,11] The Harry Dym equation is an important integrable model in soliton theory[12] and is related to the classical string problem and has many applications in theoretical and experimental physics.[13] Here in our paper, we shall use the phase analysis method of planar dynamical systems and the theory of the singular traveling wave systems[6,7,14] to find all possible bounded traveling wave solutions of Eq. (1) and their parametric representations for the cases of $k=-2,-\frac{1}{2},\frac{1}{2},2$, respectively.

Let us start from the traveling wave setting in the form $m(x,t)=\phi(\xi)$, $\xi=x-ct$, where c denotes the wave speed. Substituting this form into (1) and integrating on both sides of Eq. (1) with respect to ξ, we arrive at

---

[a)]Electronic addresses: lijb@zjnu.cn and jibinli@gmail.com.
[b)]Electronic mail: qiao@utpa.edu.

$$k\phi\phi'' = k(k+1)(\phi')^2 + 2c\phi^{k+3} - 2g\phi^{k+2} - \phi^2, \tag{2}$$

where g is an integral constant and " $'$" stands for the derivative with respect to ξ. Equation (2) can be equivalently rewritten as the following planar dynamic system:

$$\frac{d\phi}{d\xi} = y, \quad \frac{dy}{d\xi} = \frac{k(k+1)y^2 + 2\phi^2\left(c\phi^{k+1} - g\phi^k - \frac{1}{2}\right)}{k\phi}, \tag{3}$$

with the first integral

$$H_k(\phi,y) = \frac{y^2}{\phi^{2k+2}} + \frac{4c}{k(k-1)\phi^{k-1}} - \frac{4g}{k^2\phi^k} - \frac{1}{k^2\phi^{2k}} = h, \quad k \neq 1, \tag{4}$$

and

$$H_1(\phi,y) = \frac{y^2}{\phi^4} - \frac{1}{\phi^2} - \frac{4g}{\phi} - 4c\ \ln|\phi|, \quad k=1.$$

Actually, system (3) is able to be cast in the following canonical Hamiltonian system:

$$\Phi_\xi = J\frac{\partial H_k}{\partial \Phi}, \quad \Phi = (\phi,y)^T,$$

where

$$J = \begin{pmatrix} 0 & \frac{1}{2}\phi^{2k+2} \\ -\frac{1}{2}\phi^{2k+2} & 0 \end{pmatrix}, \quad \frac{\partial H_k}{\partial \Phi} = \begin{pmatrix} \frac{\partial H_k}{\partial \phi} \\ \frac{\partial H_k}{\partial y} \end{pmatrix}.$$

Notice that for $k<0$, $k\neq -1$, letting $n=-k>0$, system (3) becomes

$$\begin{cases} \dfrac{d\phi}{d\xi} = y, \quad \dfrac{dy}{d\xi} = \dfrac{-n(n-1)\phi^{n-2}y^2 + (\phi^n - 2c\phi + 2g)}{n\phi^{n-1}}, & \text{if} \quad n \geq 2 \\ \dfrac{d\phi}{d\xi} = y, \quad \dfrac{dy}{d\xi} = \dfrac{-n(n-1)y^2 + \phi^{2-n}(\phi^n - 2c\phi + 2g)}{n\phi}, & \text{if} \quad 0<n<2, \end{cases} \tag{3'}$$

with the first integral

$$H_n(\phi,y) = y^2\phi^{2n-2} + \frac{4c}{n(n+1)}\phi^{n+1} - \frac{4g}{n^2}\phi^n - \frac{1}{n^2}\phi^{2n} = h. \tag{4'}$$

Clearly, system (3) is a singular dynamical system.[7–9] The phase portraits produced by the vector fields of system (3) determine all possible traveling wave solutions $\phi(\xi)$. In what follows, we shall first investigate the dynamical behavior of the function $\phi(\xi)$ determined by system (3). Then, by using the first integral (4), we try to obtain parametric representations of all possible bounded traveling wave solutions of Eq. (1) in (c,g)-parameter plane.

Our paper is organized as follows. In Secs. II and III, we will discuss the bifurcations of phase portraits of (3) for the case $k>0$ and $k<0$, $k\neq -1$, respectively. In Secs. IV–VII, we will give the parametric representations for all possible bounded traveling wave solutions of Eq. (1) with $k=-2,-\frac{1}{2},\frac{1}{2},2$. Conclusions will be presented in Sec. VIII.

II. BIFURCATION OF PHASE PORTRAITS FOR SYSTEM (3) WHEN *k*>0

System (3) can be converted to the following associated system:

$$\frac{d\phi}{d\zeta}=ky\phi,\quad \frac{dy}{d\zeta}=k(k+1)y^2+2\phi^2\left(c\phi^{k+1}-g\phi^k-\frac{1}{2}\right). \tag{5}$$

Both systems have the same invariant curve solutions. Here $d\xi=k\phi d\zeta$ for $\phi\neq 0$.

When k is not a rational number or $k=\alpha/2l$, where the integers α and $2l$ have no common factor, we only consider the case of $\phi\geq 0$ in systems (5) and (3).

Obviously, the origin $O(0,0)$ is a high-order equilibrium point of (5) for $k>0$. By the qualitative theory of planar dynamical systems, there are two elliptic areas and four parabola areas of the orbits of (5) in a neighborhood of the origin if k is a rational number, but $k\neq\alpha/2l$.

In the case of $k=1$, because the first integral $H_1(\phi,y)$ contains a term of $\ln|\phi|$, we cannot use the first equation of (3) to give the parametric representations of the traveling wave solutions of (1). But the phase portraits of (3) may be gotten by using the procedure similar to other k's.

Let $f(\phi)=c\phi^{k+1}-g\phi^k-\frac{1}{2}$, then $f'(\phi)=\phi^{k-1}[(k+1)c\phi-kg]$. Apparently, $\phi_*=kg/(k+1)c$ is a critical number of $f(\phi)$ and $f(\phi_*)=-(g/(k+1))(kg/(k+1)c)^k-1/2$. Thus, when $g^{k+1}=-(k+1)^{k+1}c^k/2k^k$, $f(\phi_*)=0$.

Because $f'(\phi)$ has at most two zeros at 0 and ϕ_* and $f(0)=-\frac{1}{2}$. Thus, $f(\phi)=0$ has at most three roots. The exact number of the roots of $f(\phi)=0$ depends on k and the zone of the (c,g)-parameter plane. The curve given by

$$g=-\left(1+\frac{1}{k}\right)\left(\frac{kc^k}{2}\right)^{1/(k+1)} \qquad (\mathrm{BC_k})$$

is a bifurcation curve of the (c,g)-parameter plane, which may have two branches.

Let ϕ_j, $j=1,2,3$ be the roots of the equation $f(\phi)=0$. Then, $E_j(\phi_j,0)$, $j=1,2,3$ are all equilibrium points of (5). The determinant of the linearized system of (5) at $E_j(\phi_j,0)$ is $J_j=-k\phi_j^3 f'(\phi_j)$. Considering the sign of each J_j, we know that E_j is a center or a saddle point. In particular, the double equilibrium point $E_*(\phi_*,0)$ of (5) is a cusp point.

Let us now take $k=2$ and $k=\frac{1}{2}$ as two examples in order to see the dynamical behaviors of (3).

(I) The case of $k=2$. The bifurcation curves are $g=-\frac{3}{2}c^{2/3}$ and $c=0$ in the (c,g)-parameter plane.

When $k=2$, system (5) becomes

$$\frac{d\phi}{d\zeta}=y\phi,\quad \frac{dy}{d\zeta}=3y^2+\phi^2\left(c\phi^3-g\phi^2-\frac{1}{2}\right), \tag{6}$$

with the first integral,

$$H_2(\phi,y)=\frac{y^2}{\phi^6}+\frac{2c}{\phi}-\frac{g}{\phi^2}-\frac{1}{4\phi^4}=h. \tag{7}$$

A qualitative analysis may yield the following results.

(1) For $g>-\frac{3}{2}c^{2/3}$, $c>0$, there exists a uniquely elementary equilibrium point $E_1(\phi_1,0)$ of (6) with $\phi_1>0$, which is a saddle point. See the details of the corresponding phase portrait of (6) in Fig. 1 (1–1).

(2) For $g>-\frac{3}{2}c^{2/3}$, $c<0$, there exists a uniquely elementary equilibrium point $E_1(\phi_1,0)$ of (6) with $\phi_1<0$, which is also a saddle point. See the details of the corresponding phase portrait of (6) in Fig. 1 (1–2).

(3) For $g=-\frac{3}{2}c^{2/3}$, $c<0$, there exist two equilibrium points $E_1(\phi_1,0)$ and $E_*(\phi_*,0)$ of (6) with $\phi_1<0$, $\phi_*>0$. E_1 is a saddle point but E_* is a cusp point. See the details of the corresponding phase portrait of (6) in Fig. 1 (1–3).

(4) For $g<-\frac{3}{2}c^{2/3}$, $c<0$, there exist three equilibrium points $E_1(\phi_1,0)$, $E_2(\phi_2,0)$, and $E_3(\phi_3,0)$ of (6) with $\phi_1<0$, $0<\phi_2<\phi_*<\phi_3$. E_1, E_2 are saddle points but E_3 is a center. See the details of the corresponding phase portrait of (6) in Fig. 1 (1–4).

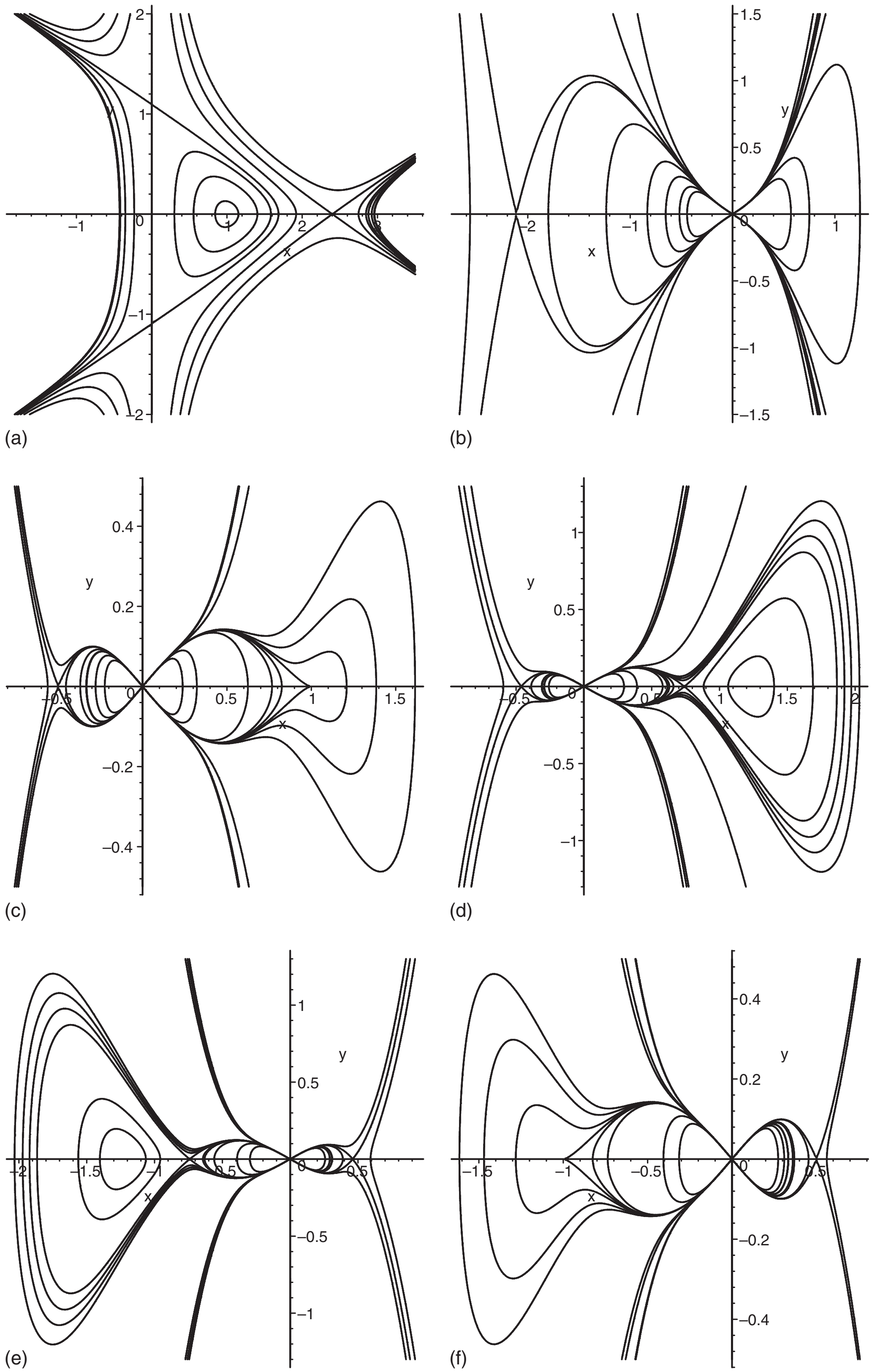

FIG. 1. The bifurcation of phase portraits of system (6) in the (c,g)-plane. (1–1) $g > -\frac{3}{2}c^{2/3}$, $c > 0$, (1–2) $g > -\frac{3}{2}c^{2/3}$, $c < 0$, (1–3) $g = -\frac{3}{2}c^{2/3}$, $c < 0$, (1–4) $g < -\frac{3}{2}c^{2/3}$, $c < 0$, (1–5) $g < -\frac{3}{2}c^{2/3}$, $c > 0$, and (1–6) $g = -\frac{3}{2}c^{2/3}$, $c > 0$.

(5) For $g<-\frac{3}{2}c^{2/3}$, $c>0$, there exist three equilibrium points $E_1(\phi_1,0)$, $E_2(\phi_2,0)$, and $E_3(\phi_3,0)$ of (6) with $\phi_1>0$, $\phi_3<\phi_*<\phi_2<0$. E_1, E_2 are saddle points while E_3 is a center. See the details of the corresponding phase portrait of (6) in Fig. 1 (1–5).

(6) For $g=-\frac{3}{2}c^{2/3}$, $c>0$, there exist two equilibrium points $E_1(\phi_1,0)$ and $E_*(\phi_*,0)$ of (6) with $\phi_1>0$, $\phi_*<0$. E_1 is a saddle point while E_* is a cusp point. See the details of the corresponding phase portrait of (6) in Fig. 1 (1–6).

(II) The case of $k=\frac{1}{2}$. The bifurcation curves are $g=-3(|c|/16)^{1/3}$ and $c=0$ in the (c,g)-parameter plane.

$k=\frac{1}{2}$ leads system (5) to be

$$\frac{d\phi}{d\zeta}=\frac{1}{2}y\phi,\quad \frac{dy}{d\zeta}=\frac{3}{4}y^2+2\phi^2\left(c\phi^{3/2}-g\sqrt{\phi}-\frac{1}{2}\right), \tag{8}$$

with the first integral,

$$H_{1/2}(\phi,y)=\frac{y^2}{\phi^3}-16c\sqrt{\phi}-\frac{16g}{\sqrt{\phi}}-\frac{4}{\phi}=h. \tag{9}$$

Apparently, $\phi>0$ is needed for us to get real solutions. Therefore, the function $f(\phi)=c\phi^{3/2}-g\sqrt{\phi}-\frac{1}{2}$ has at most two positive zeros saying ϕ_1, ϕ_2, i.e., $0<\phi_1<\phi_2$.

All the phase portraits of (8) are the same as ones shown in the right (c,g)—phase plane of Fig. 1, but under the bifurcation parameter condition $g=-3(|c|/16)^{1/3}$.

III. BIFURCATION OF PHASE PORTRAITS FOR SYSTEM (3′)

System (3′) can be changed to the following associated system:

$$\begin{cases}\dfrac{d\phi}{d\zeta}=ny\phi^{n-1}, & \dfrac{dy}{d\zeta}=-n(n-1)\phi^{n-2}y^2+(\phi^n-2c\phi+2g), \quad \text{if} \quad n\geq 2\\ \dfrac{d\phi}{d\zeta}=ny\phi, & \dfrac{dy}{d\zeta}=-n(n-1)y^2+\phi^{2-n}(\phi^n-2c\phi+2g), \quad \text{if} \quad 0<n<2.\end{cases} \tag{10}$$

Both systems have the same invariant curve solutions.

When n is not a rational number or $n=\alpha/2l$, where the integers α and $2l$ have no common factor, we only consider the case of $\phi\geq 0$ in system (10) and (3′).

Let $f_1(\phi)=\phi^n-2c\phi+2g$, then $f_1'(\phi)=n\phi^{n-1}-2c$. Apparently, $\phi_*=(2c/n)^{1/(n-1)}$ is a critical number of $f_1(\phi)$ and $f_1(\phi_*)=-[2c(n-1)/n](2c/n)^{1/(n-1)}+2g$. Thus, when $g=[(n-1)c/n]\phi_*$, $f_1(\phi_*)=0$. Because $f_1'(\phi)$ has at most two zeros and $f_1(0)=2g$, $f_1(\phi)=0$ has at most three roots. The exact number of the roots of $f_1(\phi)=0$ depends on n and the zone of the (c,g)-parameter plane. The curve given by

$$g=\frac{(n-1)c}{n}\left(\frac{2c}{n}\right)^{1/(n-1)} \qquad \text{(BCn)}$$

is a bifurcation curve of the (c,g)-parameter plane.

Let $\phi_j, j=1,2,3$ be the three roots of the equation $f_1(\phi)=0$. Then, $E_j(\phi_j,0)$ are all equilibrium points of (10). The determinants of the linearized system of (10) at $E_j(\phi_j,0)$ are $J_j=-n\phi_j^{n-1}f_1'(\phi_j)$ (for $n\geq 2$) and $J_j=-n\phi_j^{3-n}f_1'(\phi_j)$ (for $0<n<2$), respectively. Considering the sign of each J_j, we know that E_j is a center or a saddle point. In particular, the double equilibrium point $E_*(\phi_*,0)$ of (10) is a cusp point.

Let us now take $n=2$ and $n=\frac{1}{2}$ as two examples in order to see the dynamical behaviors of (3′).

(III) The case of $k=-2(n=2)$. The bifurcation curves are $g=-\frac{1}{2}c^2$, $c=0$, and $h_2=0$ (see below) in the (c,g)-parameter plane.

In this case, system (10) is reduced to

$$\frac{d\phi}{d\zeta} = 2\phi y, \quad \frac{dy}{d\zeta} = -2y^2 + (\phi^2 - 2c\phi + 2g), \tag{11}$$

with the first integral,

$$H_{-2}(\phi,y) = \phi^2 y^2 + \tfrac{2}{3}c\phi^3 - g\phi^2 - \tfrac{1}{4}\phi^4 = h. \tag{12}$$

Assume $c>0$ and let $\Delta = c^2 - 2g$. Then, when $\Delta = c^2 - 2g < 0$, system (11) has no equilibrium. When $\Delta > 0$, there exist two different equilibrium points $E_1(\phi_1,0)$ and $E_2(\phi_2,0)$ of (11), where $\phi_1 = c - \sqrt{\Delta}$, $\phi_2 = c + \sqrt{\Delta}$. When $\Delta = c^2 - 2g = 0$, there is a double equilibrium point. If $g>0$, then there are also two different equilibrium points $S_\pm(0,Y_\pm)$ of (11) with $Y_\pm = \pm\sqrt{g}$. They are two saddle points. Let

$$h_1 = H_{-2}(\phi_1,0) = \tfrac{2}{3}c^4 - \tfrac{2}{3}c^3\sqrt{\Delta} - 2gc^2 + \tfrac{4}{3}gc\sqrt{\Delta} + g^2$$

and

$$h_2 = H_{-2}(\phi_2,0) = \tfrac{2}{3}c^4 + \tfrac{2}{3}c^3\sqrt{\Delta} - 2gc^2 - \tfrac{4}{3}gc\sqrt{\Delta} + g^2.$$

Using the analysis procedure similar to the case of $k=2$, we can get the bifurcations of phase portraits of (11), which are shown in Fig. 2.

When $c<0$, the phase portraits of (11) are just the symmetric images of the phase portraits in Fig. 2 with respect to y-axis.

(IV) The case of $k=-\frac{1}{2}$ $\left(n=\frac{1}{2}\right)$. The bifurcation curves are $g=-1/16c$ and $c=0$ in the (c,g)-parameter plane.

In this case, system (10) reads as

$$\frac{d\phi}{d\zeta} = \frac{1}{2}\phi y, \quad \frac{dy}{d\zeta} = \frac{1}{4}y^2 - \phi^{3/2}(2c\phi - \sqrt{\phi} - 2g), \tag{13}$$

with the first integral,

$$H_{-1/2}(\phi,y) = \frac{y^2}{\phi} + \frac{16}{3}c\phi^{3/2} - 16g\sqrt{\phi} - 4\phi = h. \tag{14}$$

When $c>0$, $g\geq 0$, there is only one positive equilibrium point $E_2(\phi_2,0)$ of (13) with $\phi_2 = (1/16c^2)(1+\sqrt{1+16cg})^2$. When $c>0$, $-1/16c \leq g < 0$, or $c<0$, $-1/16c \geq g > 0$, there exist two positive equilibrium points $E_1(\phi_1,0)$ and $E_2(\phi_2,0)$ of (13), where $\phi_1 = (1/16c^2)(1-\sqrt{1+16cg})^2$. When $c\leq 0$, $g<0$, there is only one positive equilibrium point $E_1(\phi_1,0)$ of (13).

Let $h_j = H_{-1/2}(\phi_j,0)$, $j=1,2$. Using the analysis procedure similar to the case of $k=2$, we can get the bifurcations of phase portraits of (13), which are shown in Fig. 3.

IV. DYNAMICS OF THE LEVEL CURVES AND PARAMETRIC REPRESENTATIONS OF SOLUTIONS FOR SYSTEM (3) WITH $k=2$

Let us consider the dynamics of the level curves determined by $H_2(\phi,y)=h$. It is easy to see from Fig. 1 that figures (1–1) and (1–2), (1–3) and (1–6), and (1–4) and (1–5) are symmetric with respect to the y-axis, respectively. So, we just discuss the cases of Fig. 1, (1–1), (1–3), and (1–4).

Let $h_j = H_2(\phi_j,0)$, $j=1,2,3$ and $h_* = H_2(\phi_*,0) = (3c^2/4g)(1-27c^2/16g^3)$, where H_2 is defined by (7). For any real number h, along the level curves $H_2(\phi,y)=h$ we have

$$y^2 = \phi^2\left(\tfrac{1}{4} + g\phi^2 - 2c\phi^3 + h\phi^4\right), \tag{15}$$

which implies that the level curves $H_2(\phi,y)=h$ are sextic when $h\neq 0$.

Taking integration of (15) yields

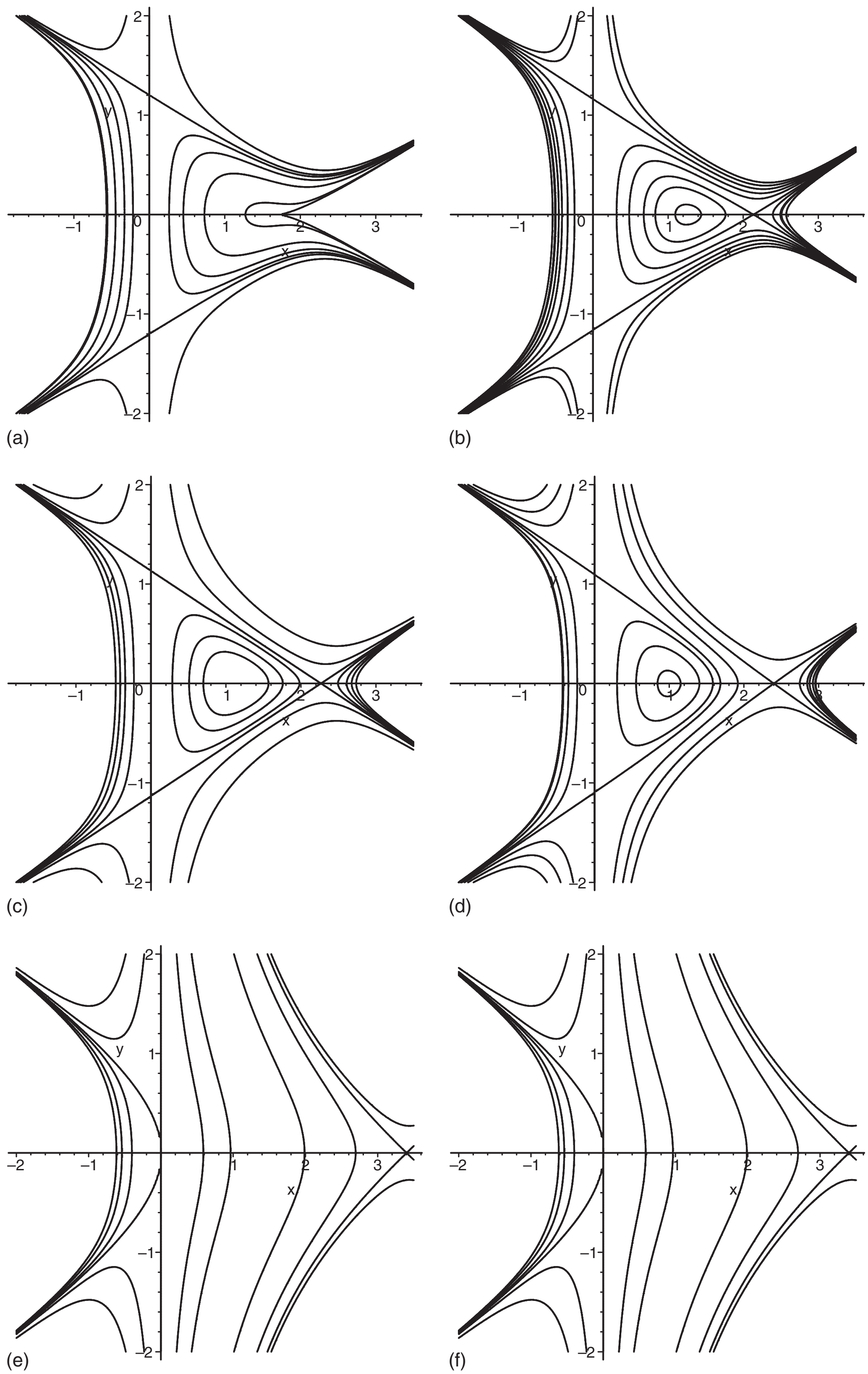

FIG. 2. The bifurcation of phase portraits of system (11) in the (c,g)-plane. (2–1) $g=c^2/2$. (2–2) $0<g<c^2/2$, $h_1<h_2<0$. (2–3) $0<g<c^2/2$, $h_1<h_2=0$. (2–4) $0<g<c^2/2$, $h_1<0<h_2$. (2–5) $g=0$. (2–6) $g<0$.

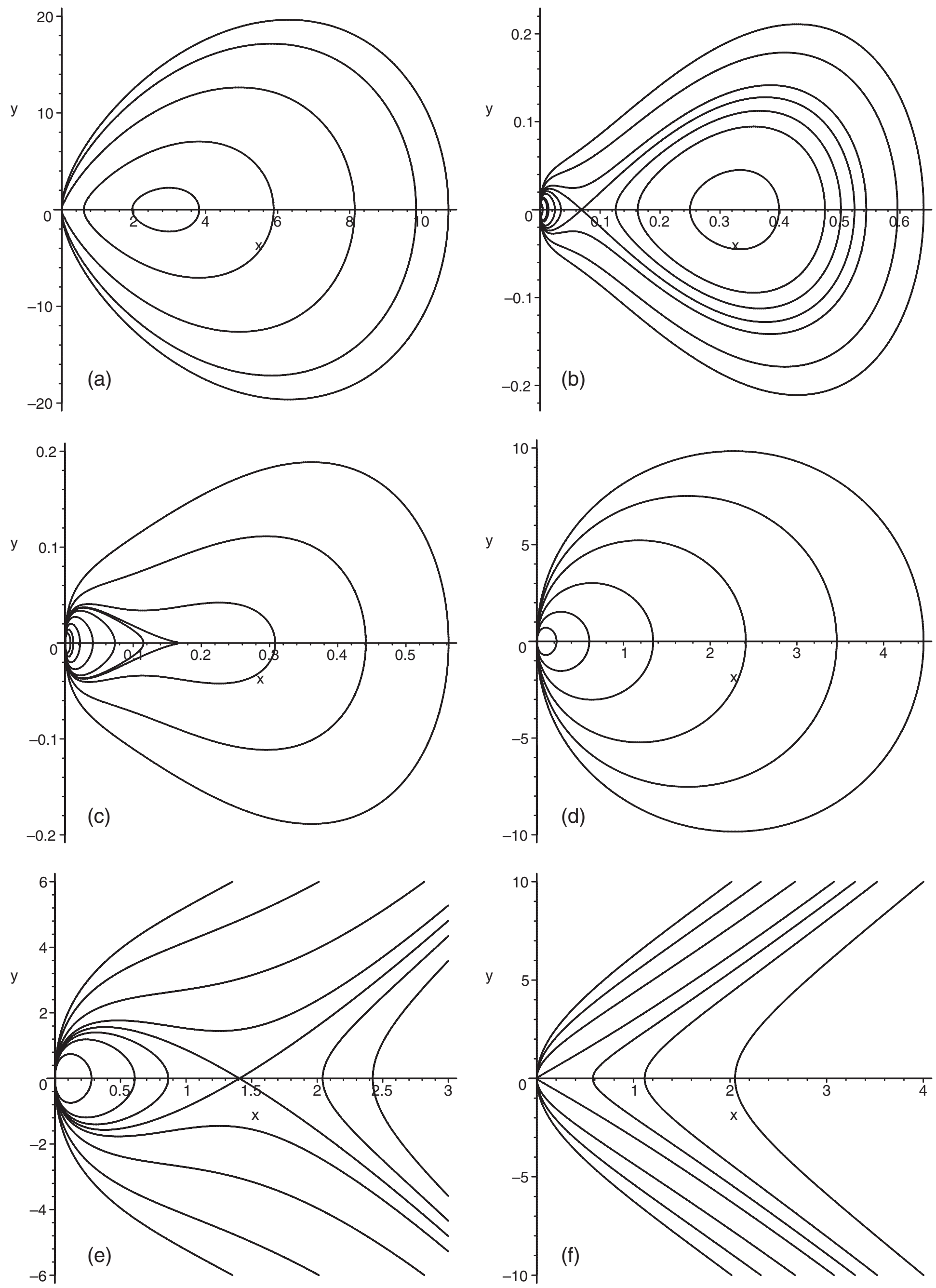

FIG. 3. The bifurcation of phase portraits of system (13) in the (c,g)-plane. (3–1) $c>0$, $g\geq 0$ (3–2) $c>0$, $-1/16c<g<0$. (3–3) $c>0$, $g=-1/16c$. (3–4) $c>0$, $g<-1/16c$. (3–5) $c\leq 0$, $g<0$. (3–6) $c\leq 0$, $g\geq 0$.

$$\int_{\phi_0}^{\phi} \frac{d\phi}{\phi\sqrt{\frac{1}{4}+g\phi^2-2c\phi^3+h\phi^4}} = \xi, \tag{16}$$

where ϕ_0 is any real number as an initial value of ϕ. The left hand side of (16) is an elliptic integral (see Ref. 15). In principle, we can use (16) to get all parametric representations of infinitely many smooth traveling wave solutions of system (1) with $k=2$. But, in general, ϕ is not able to be explicitly expressed in terms of functions of ξ. However, in very special cases of relationship between c and g, we may get explicit peakon solutions.[8,9]

Suppose $g>-\frac{3}{2}c^{2/3}$, $c>0$. Then, $H_2(\phi_1,0)=h_1>0$. We see from Fig. 1 (1–1) that the following results hold.

When $h=h_1$, the level curves $H_2(\phi,y)=h_1$ consist of six orbits of (6). Two of them are heteroclinic orbits connecting $O(0,0)$ to $E_1(\phi_1,0)$, and the remaining four are open curves [see Fig. 4 (4–2)].

The two heteroclinic orbits give rise to a kink and an antikink wave solutions of (1) with $k=2$. In order to obtain the parametric representations of the two solutions, we change Eq. (15) to

$$y = \sqrt{h_1}\phi(\phi_1 - \phi)\sqrt{A + B\phi + \phi^2}.$$

Taking integral from ϕ_0 to ϕ yields

$$\phi(\chi) = \pm \frac{4A\Phi_a}{\Phi_a^2 e^{-\chi} + \Delta_1 e^{\chi} - 2B\Phi_a},$$

$$\xi(\chi) = \frac{1}{\phi_1\sqrt{Ah_1}}\left[\chi + \sqrt{\frac{A}{\tilde{A}}}\ln\left(\frac{2\sqrt{\tilde{A}(A + B\phi(\chi) + \phi^2(\chi))} + \tilde{B}(\phi_1 - \phi(\chi)) + 2\tilde{A}}{\phi_1 - \phi(\chi)}\right) - \Psi_a\right], \tag{17}$$

where A, B are two constants, $0<\phi_0<\phi_1$, $\tilde{A}=A+B\phi_1+\phi_1^2$, $\tilde{B}=-(B+2\phi_1)$, $\Delta_1=B^2-4A<0$, $\Phi_a=(2\sqrt{A(A+b\phi_0+\phi_0^2)}+B\phi_0+2A)/\phi_0$, and $\Psi_a=\sqrt{\frac{A}{\tilde{A}}}\ln((2\sqrt{\tilde{A}(A+B\phi_0+\phi_0^2)}+\tilde{B}(\phi_1-\phi_0)+2\tilde{A})/(\phi_1-\phi_0))$.

When $h\in[0,h_1)$, there is a family of homoclinic orbits determined by $H_2(\phi,y)=h$ [see Fig. 4 (4–3)]. These homoclinic orbits lead to infinitely many smooth solitary wave solutions of Eq. (1) ($k=2$) with positive amplitudes [see Fig. 5 (5–1)]. The maximum of solitary waves $\phi(\xi)$ is not more than ϕ_1.

When $h\in(-\infty,0)$, there are two families of homoclinic orbits with "∞-shape" determined by $H_2(\phi,y)=h$ [see Fig. 4 (4–4)]. Corresponding to these orbits, there exist infinitely many smooth solitary wave solutions, see Fig. 5, (5–1) and (5–2). As $h\to\infty$, the amplitudes of waves tend to zero.

Suppose $g=-\frac{3}{2}c^{2/3}$, $c<0$. Then, $h_1=H_2(\phi_1,0)>0$ and $h_*=-\frac{3}{4}c^{4/3}<0$.

When $h=h_1$, the level curves $H_2(\phi,y)=h_1$ consist of six orbits of (6). Two of them are heteroclinic orbits, which connect $O(0,0)$ to $E_1(\phi_1,0)$, and the remaining four are open curves [see Fig. 6 (6–2)]. The two heteroclinic orbits lead to a kink and an antikink wave solutions of (1) with $k=2$, which possess the following parametric representations:

$$\phi(\chi) = \mp \frac{4A\Phi_a}{\Phi_a^2 e^{-\chi} + \Delta_1 e^{\chi} - 2B\Phi_a},$$

$$\xi(\chi) = \frac{1}{\phi_1\sqrt{Ah_1}}\left[\chi + \sqrt{\frac{A}{\tilde{A}}}\ln\left(\frac{2\sqrt{\tilde{A}(A + B\phi(\chi) + \phi^2(\chi))} + \tilde{B}(\phi_1 - \phi(\chi)) + 2\tilde{A}}{\phi_1 - \phi(\chi)}\right) - \Psi_a\right], \tag{18}$$

where $\phi_1<\phi_0<0$ and other constants are the same as (17).

When $h\in(0,h_1)$, there exists a family of homoclinic orbits determined by $H_2(\phi,y)=h$ [see Fig. 6 (6–3)]. These homoclinic orbits yield infinitely many smooth solitary wave solutions of (1) ($k=2$) with the negative amplitudes [see Fig. 5 (5–1)]. The maximum of solitary waves $\phi(\xi)$ is not more than $|\phi_1|$.

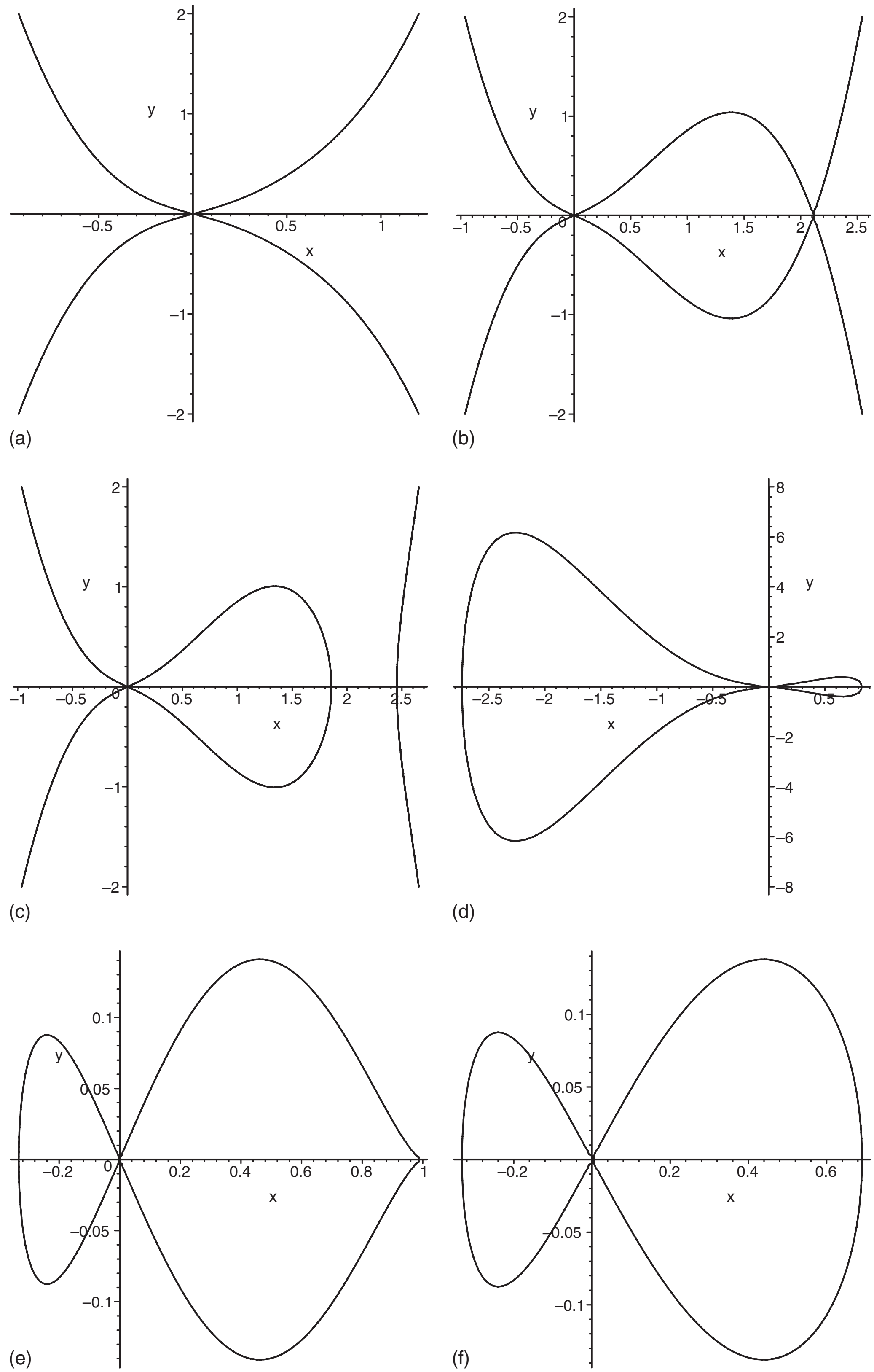

FIG. 4. The level curves defined by $H_2(\phi, y) = h$ of system (6).

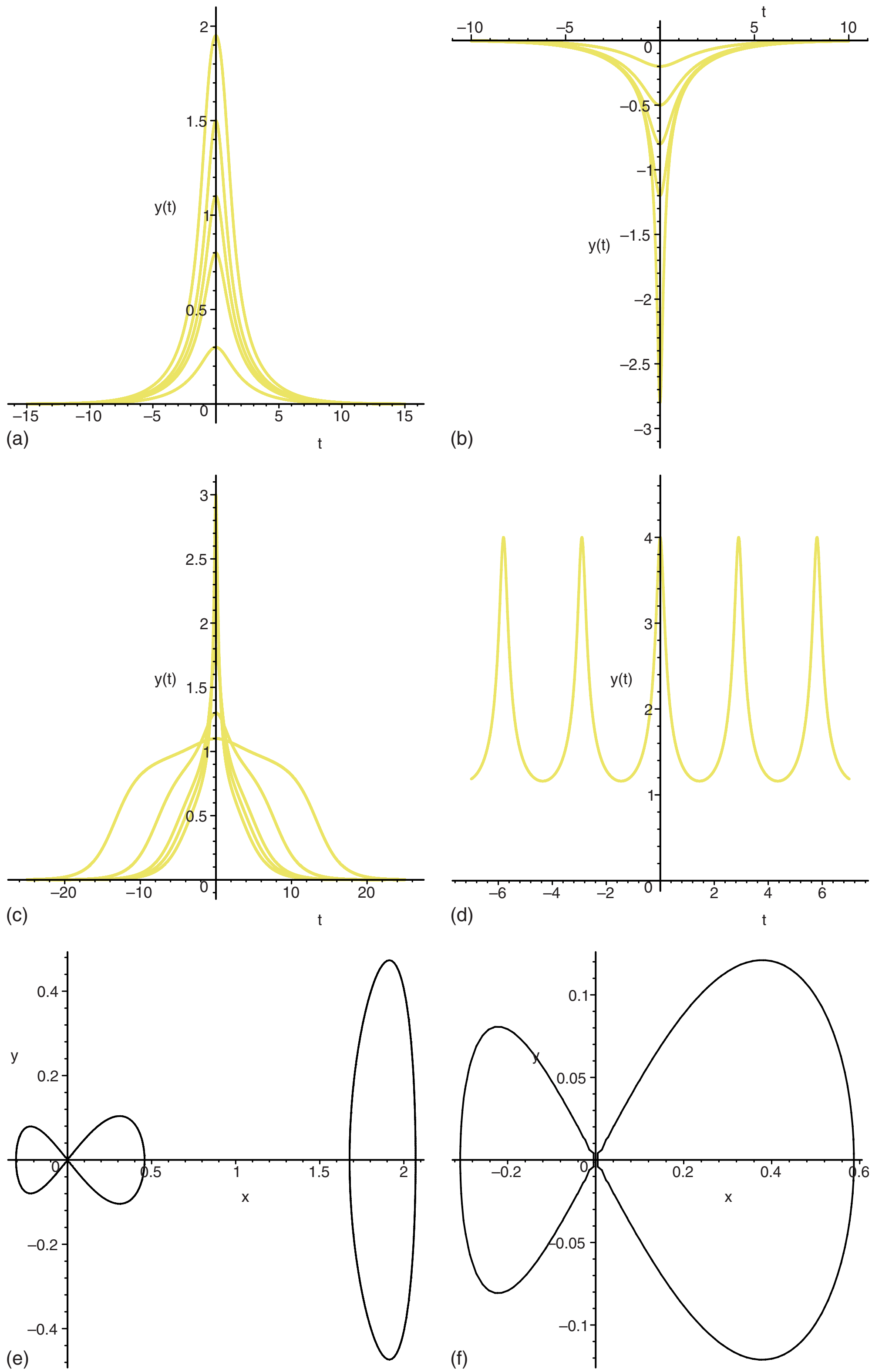

FIG. 5. (Color online) The profiles of solitary waves and periodic waves of (1) with $k=2$. (5–1) When $g=2$, $c=1$, uncountably infinite many solitary wave solutions of peak type of (1). (5–2) When $g=2$, $c=1$, uncountably infinite many solitary wave solutions of valley type of (1). (5–3) $g=-\frac{3}{2}$, $c=1$, uncountably infinite many solitary wave solutions of peak type of (1). (5–4) $g=-2$, $c=-1$, a periodic wave solution.

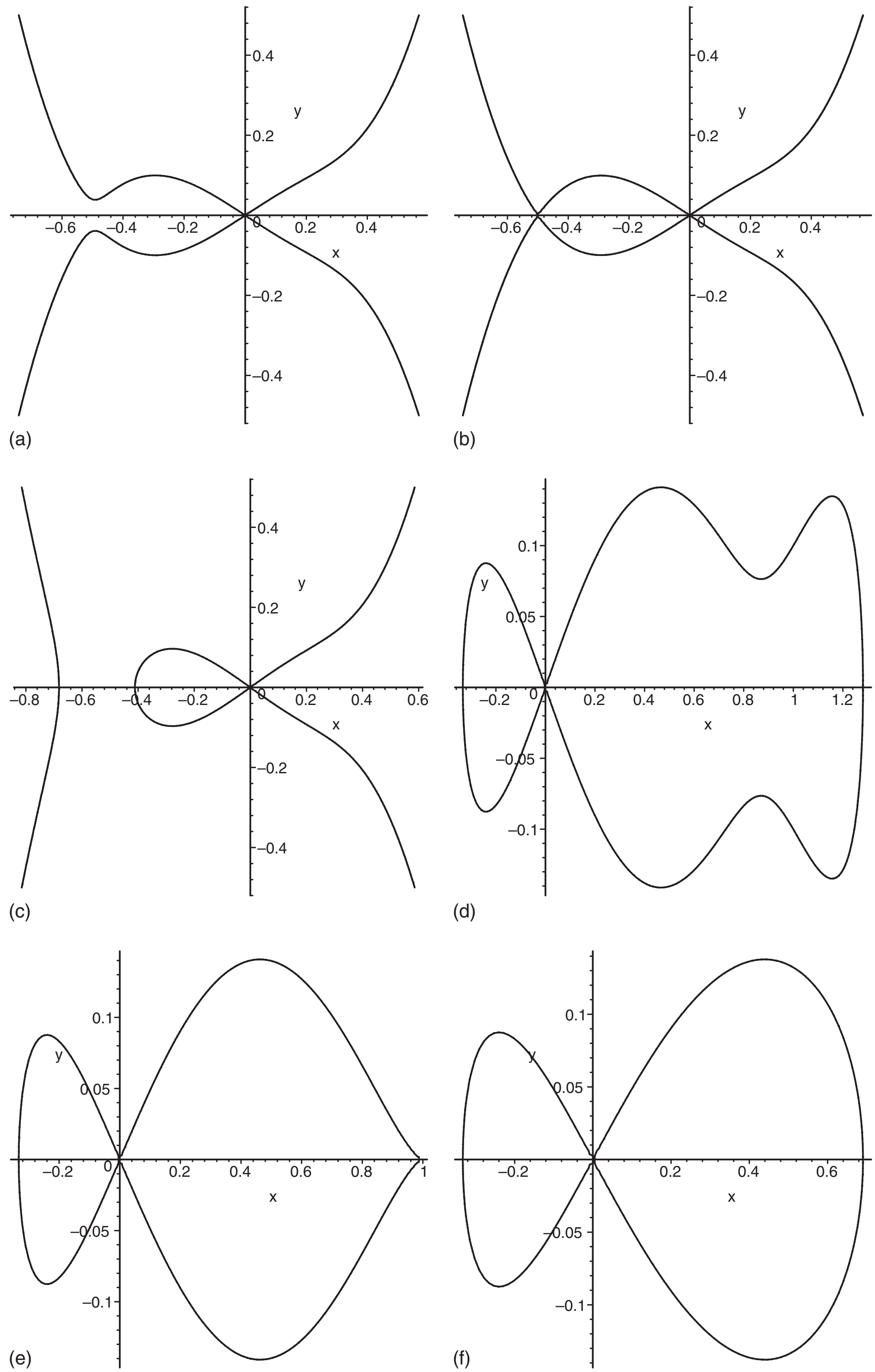

FIG. 6. The level curves of defined by $H_2(\phi,y)=h$ of system (6).

When $h \in (h_*, 0)$, there exist two families of homoclinic orbits determined by $H_2(\phi, y) = h$ [see Fig. 6 (6–4)]. For a given h, the orbit in the right phase plane is a larger loop while the one in the left phase plane is a smaller loop. Corresponding to these orbits, there are infinitely many smooth solitary wave solutions with positive and negative amplitudes, see Fig. 5, (5–3) and (5–2).

When $h = h_*$, the level curves $H_2(\phi, y) = h_*$ consist of three orbits of (6). Two of them are heteroclinic orbits, which connects $O(0,0)$ to $E_*(\phi_*, 0)$, and the third one is a homoclinic orbit in the left phase plane [see Fig. 6 (6–5)]. The two heteroclinic orbits determined by $H_2(\phi, y) = h_*$, i.e., $y = \sqrt{|h_*|}\phi(\phi_* - \phi)\sqrt{A + B\phi - \phi^2}$ give rise to a kink and an antikink wave solution of (1) with $k=2$, which have the parametric representations,

$$\phi(\chi) = \pm \frac{4A\Phi_a}{\Phi_a^2 e^{-\chi} + \Delta_1 e^{\chi} - 2B\Phi_a},$$

$$\xi(\chi) = \frac{1}{\phi_1\sqrt{A|h_*|}}\left[\chi + \sqrt{\frac{A}{\tilde{A}}}\ln\left(\frac{2\sqrt{\tilde{A}(A + B\phi(\chi) + \phi^2(\chi))} + \tilde{B}(\phi_* - \phi(\chi)) + 2\tilde{A}}{\phi_* - \phi(\chi)}\right) - \Psi_a\right], \tag{19}$$

where A, B are two constants, $0 < \phi_0 < \phi_*$, $\tilde{A} = A + B\phi_* + \phi_*^2$, $\tilde{B} = -(B + 2\phi_*)$, $\Delta_1 = B^2 - 4A > 0$, $\Phi_a = (2\sqrt{A(A + b\phi_0 + \phi_0^2)} + B\phi_0 + 2A)/\phi_0$, and $\Psi_a = \sqrt{\frac{A}{\tilde{A}}}\ln((2\sqrt{\tilde{A}(A + B\phi_0 + \phi_0^2)} + \tilde{B}(\phi_* - \phi_0) + 2\tilde{A})/(\phi_* - \phi_0))$.

When $h \in (-\infty, h_*)$, the level curves determined by $H_2(\phi, y) = h$ are two families of homoclinic orbits of (6) with "∞-shape" [see Fig. 6 (6–6)]. Corresponding to these orbits, there exist infinitely many smooth solitary wave solutions with positive and negative amplitudes, see Fig. 5, (5–1) and (5–2).

Suppose $g < -\frac{3}{2}c^{2/3}$, $c < 0$. Then either $h_3 < h_* < h_2 < 0 < h_1$ or $h_3 < h_* < 0 < h_2 < h_1$. We consider the former: $h_3 < h_* < h_2 < 0 < h_1$. The latter is similar.

When $h = h_1$, the level curves $H_2(\phi, y) = h_1$ still consist of six orbits of (6). Two of them are heteroclinic orbits, which connects $O(0,0)$ to $E_1(\phi_1, 0)$, and the remaining four are open curves [see Fig. 7 (7–1)]. The two heteroclinic orbits yield a kink and an antikink wave solutions of (1) with $k=2$, which possess the same parametric representations as (11).

When $h \in (0, h_1)$, there exists a family of homoclinic orbits of (6), which is determined by $H_2(\phi, y) = h$ to the origin $O(0,0)$ [see Fig. 7 (7–2)]. These homoclinic orbits lead to infinitely many solitary wave solutions of (1) ($k=2$) with negative amplitude [see Fig. 5 (5–1)]. The maximum of solitary waves $\phi(\xi)$ is not more than $|\phi_1|$.

When $h \in (h_2, 0)$, the level curves $H_2(\phi, y) = h_2$ consist of two families of homoclinic orbits of (6) with "∞-shape" [see Fig. 7 (7–3)]. Therefore, two families of homoclinic orbits yield two families of smooth solitary wave solutions with positive and negative amplitudes, respectively, see Fig. 5, (5–1) and (5–2).

When $h = h_2$, the level curves determined by $H_2(\phi, y) = h_2$ are two homoclinic orbits of (6) connecting the origin $O(0,0)$ to E_1 [see Fig. 7 (7–4)]. Corresponding to the homoclinic orbit passing through the point $E_2(\phi_2, 0)$ in the right phase plane, there exists a smooth solitary wave solution with positive amplitude. In fact, the current $H_2(\phi, y) = h_2$ can be written as $y = \sqrt{h_2}\phi(\phi - \phi_2)\sqrt{(\phi_M - \phi)(\phi - \phi_m)}$, where $(\phi_m, 0)$ and $(\phi_M, 0)$ are the intersection points of the two homoclinic orbits with the ϕ-axis. Taking integral from ϕ_0 to ϕ like Eq. (16) yields the following parametric representation:

$$\phi(\chi) = \frac{2|\phi_m|\phi_M}{((\phi_M + |\phi_m|)\cosh(\chi) - (\phi_M - |\phi_m|))},$$

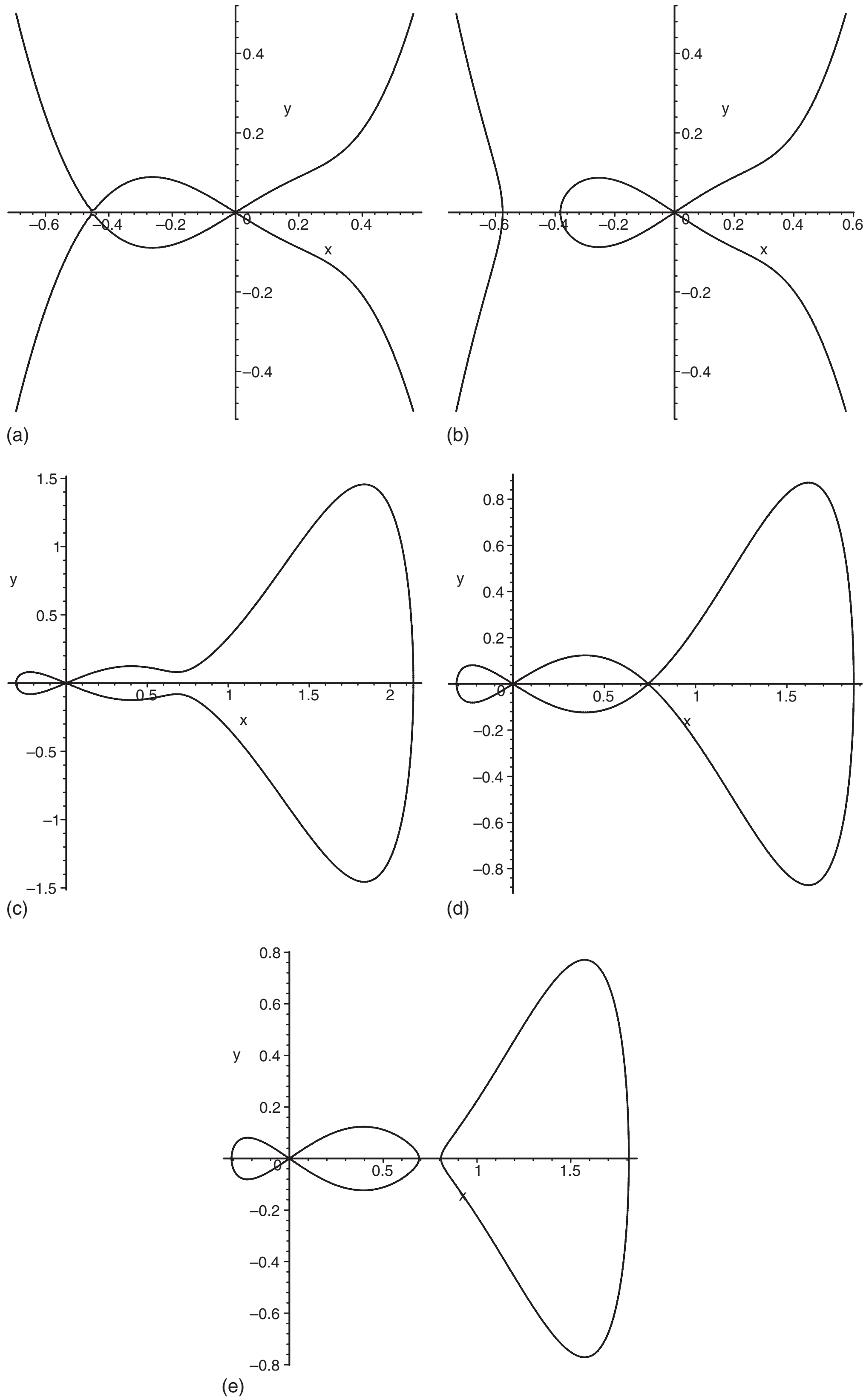

FIG. 7. The level curves of defined by $H_2(\phi, y)=h$ of system (6).

$$\xi(\chi) = \frac{1}{\phi_2\sqrt{|\phi_m|\phi_M h_2}}\left[\chi + \sqrt{\frac{|\phi_m|\phi_M}{\tilde{A}}} \times \ln\left(\frac{2\sqrt{\tilde{A}(|\phi_m|\phi_M + (\phi_M - |\phi_m|)\phi(\chi) + \phi^2(\chi))} + \tilde{B}(\phi(\chi) - \phi_2) + 2|\tilde{A}}{\phi(\chi) - \phi_2}\right) - \Psi_b\right], \tag{20}$$

where $\phi_2 < \phi_0 < \phi_M$, $\tilde{A} = |\phi_m|\phi_M + (\phi_M - |\phi_m|)\phi_2 - \phi_2^2$, $\tilde{B} = \phi_m|\phi_m| + 2\phi_2$, and $\Psi_b = \sqrt{\phi_M|\phi_m|/\tilde{A}} \times \ln((\tilde{B}(\phi_0 - \phi_2) + 2\tilde{A})/(\phi_0 - \phi_2))$.

Corresponding to the homoclinic orbit passing through the origin $O(0,0)$ in the left phase plane, there exists a smooth solitary wave solution with negative amplitude with the following parametric representation:

$$\phi(\chi) = -\frac{2|\phi_m|\phi_M}{(\phi_M + |\phi_m|)\cosh(\chi) + (\phi_M - |\phi_m|)},$$

$$\xi(\chi) = \frac{1}{\phi_2\sqrt{|\phi_m|\phi_M h_2}}\left[\chi + \sqrt{\frac{|\phi_m|\phi_M}{\tilde{A}}} \times \ln\left(\frac{2\sqrt{\tilde{A}(|\phi_m|\phi_M + (\phi_M - |\phi_m|)\phi(\chi) + \phi^2(\chi))} + \tilde{B}(\phi(\chi) - \phi_2) + 2|\tilde{A}}{\phi(\chi) - \phi_2}\right) - \Psi_b\right], \tag{21}$$

where $\phi_m < \phi_0 < 0$, $\tilde{A} = |\phi_m|\phi_M + (\phi_M - |\phi_m|)\phi_2 - \phi_2^2$, $\tilde{B} = \phi_m|\phi_m| + 2\phi_2$, and $\Psi_b = \sqrt{\phi_M|\phi_m|/\tilde{A}}\ \ln((\tilde{B}(\phi_0 - \phi_2) + 2\tilde{A})/(\phi_0 - \phi_2))$.

(20) and (21) are also kink or antikink solutions. So, two heteroclinic orbits determined by $H_2(\phi, y) = h_2$ also give rise to a kink and an antikink wave solution of (1) with $k=2$.

When $h \in (h_3, h_2)$, the level curves determined by $H_2(\phi, y) = h$ are two families of homoclinic orbits of (6) with "∞-shape" and one family of periodic orbits enclosing the equilibrium point $E_3(\phi_3, 0)$ [see Fig. 7 (7–5)]. Corresponding to the homoclinic orbits, there are infinitely many smooth solitary wave solutions with positive and negative amplitudes. Corresponding to the periodic orbits, there exist infinitely many periodic wave solutions of (1) with $k=2$ [see Fig. 3 (3–1), (3–2), and (3–4)].

When $h \in (-\infty, h_3)$, the level curves determined by $H_2(\phi, y) = h$ are two families of homoclinic orbits of (6) with "∞-shape" [see Fig. 7 (7–6)]. Corresponding to these orbits, there exist infinitely many solitary wave solutions with positive and negative amplitudes, see Fig. 5 (5–1) and (5–2).

V. DYNAMICS OF THE LEVEL CURVES AND PARAMETRIC REPRESENTATIONS OF SOLUTIONS FOR SYSTEM (3) WITH $k=\frac{1}{2}$

Let us now consider the dynamics of the level curves in Fig. 1 (1–1), (1–3), and (1–4) determined by $H_{1/2}(\phi, y) = h$ shown in Fig. 1 (1–1), (1–3), and (1–4).

Let $h_j = H_{1/2}(\phi_j, 0)$, $j = 1, 2$, and $h_* = H_{1/2}(g/3c, 0)$, where $H_{1/2}(\phi, y)$ is given by (9). For each given real number h, along the level curves determined by $H_{1/2}(\phi, y) = h$, we have

$$y^2 = \phi^2(16c\phi\sqrt{\phi} + h\phi + 16g\sqrt{\phi} - 4). \tag{22}$$

Taking integral on both sides of (22) leads to

$$\int_{\phi_0}^{\phi} \frac{d\phi}{\phi\sqrt{16c\phi\sqrt{\phi}+h\phi+16g\sqrt{\phi}-4}} = \xi, \tag{23}$$

where $\phi_0 > 0$ is an initial value.

Suppose $g > -3(c/16)^{1/3}$, $c > 0$. Then, $H_{1/2}(\phi_1,0)=h_1<0$ [see Fig. 1 (1–1)].

When $h=h_1$, the two heteroclinic orbits determined by the level curves $H_{1/2}(\phi,y)=h_1$ yield a kink and an antikink wave solutions of (1) with $k=\frac{1}{2}$. Let $\phi=\psi^2$. Then (22) can be rewritten as $y=\psi^2(\sqrt{\phi_1}-\psi)\sqrt{\psi+\sqrt{\phi_m}}$, which can be solved with the following parametric representations:

$$\phi(\chi) = \phi_m \operatorname{sech}^4(\chi),$$

$$\xi(\chi) = \pm \frac{1}{\phi_m^{1/2}\sqrt{c\phi_1}}\left[-\chi + \frac{\phi_m^{1/4}}{\sqrt{\sqrt{\phi_1}+\sqrt{\phi_m}}}\operatorname{arctanh}\left(\sqrt{\frac{\sqrt{\phi_m}(1+\operatorname{sech}^2(\chi))}{\sqrt{\phi_1}+\sqrt{\phi_m}}}\right) - \Psi_c\right], \tag{24}$$

where $-\phi_m < 0 < \phi_0 < \phi_1$ and

$$\Psi_c = -\operatorname{arctanh}\left(\sqrt{\frac{\sqrt{\phi_0}+\sqrt{\phi_m}}{\phi_m^{1/4}}}\right) + \frac{\phi_m^{1/4}}{\sqrt{\sqrt{\phi_1}+\sqrt{\phi_m}}}\operatorname{arctanh}\sqrt{\frac{\sqrt{\phi_0}+\sqrt{\phi_m}}{\sqrt{\phi_1}+\sqrt{\phi_m}}}.$$

When $h \in (-\infty, h_1)$, there are infinitely many homoclinic orbits determined by $H_{1/2}(\phi,y)=h$ and, Eq. (1) with $k=\frac{1}{2}$ has infinitely many smooth solitary wave solutions.

Suppose $g=-3(c/16)^{1/3}$, $c<0$. Then $H_{1/2}(\phi_*,0)=h_*>0$ [see Fig. 1 (1–3)].

When either $h \in (h_*,\infty)$ or $h \in (-\infty,h_*)$, there are infinitely many homoclinic orbits determined by $H_{1/2}(\phi,y)=h$, and, Eq. (1) with $k=\frac{1}{2}$ has infinitely many smooth solitary wave solutions.

When $h=h_*$, the level curves, determined by $H_{1/2}(\phi,y)=h_*$, consist of two heteroclinic orbits connecting the origin to $E_*(g/3c,0)$. In this case, we have a kink and an antikink wave solutions of (1) with $k=\frac{1}{2}$, which possess the following parametric representations:

$$\phi(\chi) = \phi_m \operatorname{sech}^4(\chi),$$

$$\xi(\chi) = \pm \frac{1}{\phi_m^{1/4}\sqrt{c\phi_*}}\left[-\chi + \frac{\phi_m^{1/4}}{\sqrt{\sqrt{\phi_*}+\sqrt{\phi_m}}}\operatorname{arctanh}\left(\sqrt{\frac{\sqrt{\phi_m}(1+\operatorname{sech}^2(\chi))}{\sqrt{\phi_*}+\sqrt{\phi_m}}}\right) - \Psi_d\right], \tag{25}$$

where $-\phi_m < 0 < \phi_0 < \phi_*$ and

$$\Psi_d = -\operatorname{arctanh}\left(\sqrt{\frac{\sqrt{\phi_0}+\sqrt{\phi_m}}{\phi_m^{1/4}}}\right) + \frac{\phi_m^{1/4}}{\sqrt{\sqrt{\phi_*}+\sqrt{\phi_m}}}\operatorname{arctanh}\sqrt{\frac{\sqrt{\phi_0}+\sqrt{\phi_m}}{\sqrt{\phi_*}+\sqrt{\phi_m}}}.$$

Suppose $g < -3(\frac{c}{16})^{1/3}$, $c<0$. Then, $y=\psi^2(\psi-\sqrt{\phi_1})\sqrt{\sqrt{\phi_M}-\psi}$, $0<\phi_1<\phi_*<\phi_2<\phi_M$, $h_1 = H_{1/2}(\phi_1,0) > H_{1/2}(\phi_2,0)=h_2>0$ [see Fig. 1 (1–4)].

When either $h \in (h_1,\infty)$ or $h \in (-\infty,h_1)$, there are infinitely many homoclinic orbits determined by $H_{1/2}(\phi,y)=h$, and, Eq. (1) with $k=\frac{1}{2}$ has infinitely many smooth solitary wave solutions.

When $h=h_1$, the level curves, determined by $H_{1/2}(\phi,y)=h_1$, consist of two heteroclinic orbits connecting the origin to $E_*(g/3c,0)$ and one homoclinic orbit with the saddle point $E_1(\phi_1,0)$. In this case, we have a kink and an antikink wave solutions of (1) with $k=\frac{1}{2}$, which possess the following parametric representations:

$$\phi(\chi) = \phi_M \operatorname{sech}^4(\chi),$$

$$\xi(\chi) = \mp \frac{1}{\phi_M^{1/4}\sqrt{c\phi_1}}\left[\chi + \frac{\phi_M^{1/4}}{\sqrt{\sqrt{\phi_M}-\sqrt{\phi_1}}}\operatorname{arctanh}\left(\frac{\phi_M^{1/4}\tanh(\chi)}{\sqrt{\sqrt{\phi_M}-\sqrt{\phi_1}}}\right) - \Psi_e\right], \tag{26}$$

where $0<\phi_0<\phi_1$ and

$$\Psi_e = -\operatorname{arctanh}\left(\sqrt{\frac{\sqrt{\phi_M}-\sqrt{\phi_0}}{\phi_M^{1/4}}}\right) - \frac{\phi_M^{1/4}}{\sqrt{\sqrt{\phi_M}-\sqrt{\phi_1}}}\operatorname{arctanh}\sqrt{\frac{\sqrt{\phi_M}-\sqrt{\phi_0}}{\sqrt{\phi_M}-\sqrt{\phi_1}}}.$$

In addition, we also have a smooth solitary wave solution with the following parametric representation:

$$\phi(\chi) = [\sqrt{\phi_1} + (\sqrt{\phi_M}-\sqrt{\phi_1})\operatorname{sech}^2(\chi)]^2,$$

$$\xi(\chi) = \frac{1}{\sqrt{c\phi_1(\sqrt{\phi_M}-\sqrt{\phi_1})}}\left[\chi + \sqrt{1-\sqrt{\frac{\phi_1}{\phi_M}}}\operatorname{arctanh}\left(\sqrt{1-\sqrt{\frac{\phi_1}{\phi_M}}}\tanh(\chi)\right)\right], \tag{27}$$

where we take $\phi_0=\phi_M$.

When $h\in(h_2,h_1)$, the level curves determined by $H_{1/2}(\phi,y)=h$ yield infinitely many periodic orbits enclosing the equilibrium point $E_2(\phi_2,0)$. In this case, we have infinitely many periodic wave solutions of (1) with $k=\frac{1}{2}$.

VI. DYNAMICS OF THE LEVEL CURVES AND PARAMETRIC REPRESENTATIONS OF SOLUTIONS FOR SYSTEM (3′) WITH *n*=2

In this section, we consider dynamics of the level curves in Fig. 2 (2–2)–(2–5) determined by $H_{-2}(\phi,y)=h$. For each given real number h, along the level curves, we have $y^2=(4h+4g\phi^2-\frac{8}{3}\phi^3+\phi^4)/4\phi^2$. Taking integration on both sides of the equation yields

$$\int_{\phi_0}^{\phi}\frac{\phi d\phi}{\sqrt{4h+4g\phi^2-\frac{8}{3}\phi^3+\phi^4}} = \frac{1}{2}\xi, \tag{28}$$

where ϕ_0 is an initial value.

Suppose $0<g<c^2/2$, $h_1<h_2<0$ [see Fig. 2 (2–1)], then we have the following results.

When $h\in(h_1,h_2)$, the level curves, determined by $H_{-2}(\phi,y)=h$, produce infinitely many periodic orbits enclosing the equilibrium point $E_1(\phi_1,0)$. In this case, we have infinitely many periodic wave solutions of (1) with $k=-2$, which possess the following parametric representations:

$$\phi(\chi) = r_3 + \frac{\alpha_{03}^2(r_3-r_4)\operatorname{sn}^2(\chi,k)}{1-\alpha_{03}^2\operatorname{sn}^2(\chi,k)},$$

$$\xi(\chi) = x - ct = \frac{2}{\sqrt{(r_1-r_3)(r_2-r_4)}}[r_4\chi + (r_3-r_4)\Pi(\arcsin(\operatorname{sn}(\chi,k)),\alpha_{03}^2,k)], \tag{29}$$

where $\alpha_{03}^2=(r_2-r_3)/(r_2-r_4)$, $k^2=(r_2-r_3)(r_1-r_4)/(r_2-r_4)(r_1-r_3)$, Π is the elliptic integral of the third kind, and $4h+4g\phi^2-\frac{8}{3}c\phi^3+\phi^4=(r_1-\phi)(r_2-\phi)(\phi-r_3)(\phi-r_4)$.

When $h=h_2$, the level curves determined by $H_{-2}(\phi,y)=h_2$ are the homoclinic orbit enclosing $E_2(\phi_2,0)$. In this case, there exists a smooth solitary wave solution of (1) with $k=-2$, which has the following parametric representation:

$$\phi(\chi) = \phi_2 - \frac{2(\phi_2-\phi_m)(\phi_2+\phi_4)}{(\phi_2+\phi_4)\cosh(\sqrt{(\phi_2-\phi_m)(\phi_2+\phi_4)}\chi) + (2\phi_2-\phi_m+\phi_4)},$$

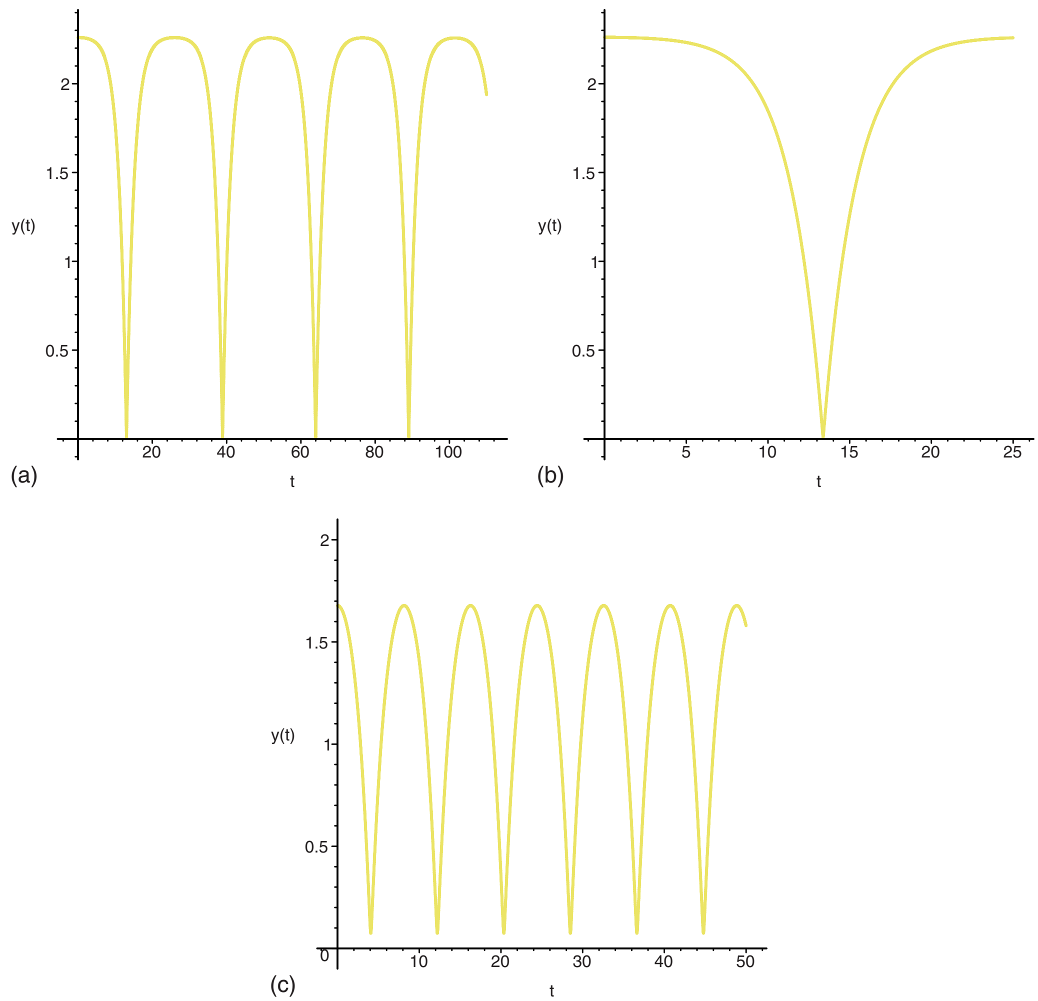

FIG. 8. (Color online) The profiles of periodic cusp waves and peakon wave of (1) with $k=-2$.

$$\xi(\chi) = 2\left[\phi_2\chi - \ln\left(\phi(\chi) + \sqrt{(\phi(\chi)-\phi_m)(\phi(\chi)+\phi_4)} + \phi(\chi) - \tfrac{1}{2}(\phi_m-\phi_4)\right) + \Phi_{01}\right], \tag{30}$$

where $\Phi_{01}=\ln\left(\phi_m-\frac{1}{2}(\phi_2-\phi_4)\right)$ and $4h+4g\phi^2-\frac{8}{3}c\phi^3+\phi^4=(\phi_2-\phi)^2(\phi-\phi_m)(\phi+\phi_4)$.

Suppose $0<g<c^2/2$, $h_1<h_2=0$ [see Fig. 2 (2–3)], then we have the following results.

When $h\in(h_1,0)$, the level curves, determined by $H_{-2}(\phi,y)=h$, are a family of periodic orbits enclosing the equilibrium point $E_1(\phi_1,0)$. In this case, we have infinitely many smooth periodic wave solutions of (1) with $n=2$, which possess the same parametric representation as the one shown in Eq. (29).

Remark: It is easy to see $k\to 1$ as $h\to 0$, r_3, $r_4\to 0$ in (29). Thus, as h approaches 0, the periodic orbit, determined by $H_{-2}(\phi,y)=h$, yields periodic cusp wave solutions [see Fig. 8 (8–1) and (8–3)].

When $h=h_2=0$, solving $H_{-2}(\phi,y)=0$ for y gives $y^2=4g^2(1-(1/\phi_2)\phi)(-1+(1/\phi_2)\phi)$. Hence, we obtain the following peakon solution [see Fig. 8 (8–2)]:

$$\phi(\xi) = \phi_2(1-e^{-2g|\xi|}). \tag{31}$$

Suppose $0<g<c^2/2$, $h_1<0<h_2$ [see Fig. 2 (2–4)], then we have the following results.

When $h\in(h_1,0)$, the level curves, determined by $H_{-2}(\phi,y)=h$, are a family of periodic orbits enclosing the equilibrium point $E_1(\phi_1,0)$. In this case, we have infinitely many smooth periodic wave solutions of (1) with $n=2$, which possess the same parametric representation as the one in (29).

When $h=0$, solving equation $H_{-2}(\phi,y)=0$ for y leads to $y^2=\frac{1}{4}(4g-\frac{8}{3}c\phi+\phi^2)=\frac{1}{4}(\phi_a-\phi)(\phi_M-\phi)$. Taking integration, we obtain the following periodic cusp wave solution [see Fig. 8 (8–3)]:

$$\phi(\xi)=\frac{1}{2}\left(\frac{8}{3}c-\sqrt{\Delta_1}\cosh\frac{1}{2}\xi\right),\quad \xi\in\left(0,2\,\text{arccosh}\left(\frac{8c}{3\sqrt{\Delta_1}}\right)\right), \tag{32}$$

where $\Delta_1=\frac{16}{9}(4c^2-9g)$.

Suppose $c>0$, $g<0$ [see Fig. 2 (2–6)], then we have the following results.

When $h\in(0,h_1)$, two branches of the level curves determined by $H_{-2}(\phi,y)=h$ are two open orbits lying in the left side and right side of the straight line $\phi=0$. In this case, we are able to factor $4h+4g\phi^2-\frac{8}{3}c\phi^3+\phi^4=(r_1-\phi)(r_2-\phi)(\phi-r_3)(\phi-r_4)$. Therefore, integrating the first equation of (3′) generates the parametric representations of the two breaking wave solutions of Eq. (1) with $n=-k=2$,

$$\phi(\chi)=r_1-\frac{(r_1-r_2)}{1-\alpha_1^2\,\text{sn}^2(\chi,k_1)},\quad \chi\in(-\chi_{10},\chi_{10}),$$

$$\xi(\chi)=g_1[r_1\chi-(r_1-r_2)\Pi(\arcsin(\text{sn}(\chi,k_1)),\alpha_1^2,k_1)], \tag{33}$$

and

$$\phi(\chi)=r_4+\frac{(r_3-r_4)}{1-\alpha_2^2\text{sn}^2(\chi,k_1)},\quad \chi\in(-\chi_{20},\chi_{20}),$$

$$\xi(\chi)=g_1[r_4\chi+(r_3-r_4)\Pi(\arcsin(\text{sn}(\chi,k_1)),\alpha_2^2,k_1)], \tag{34}$$

where $k_1^2=(r_2-r_3)(r_1-r_4)/(r_1-r_3)(r_2-r_4)$, $\alpha_1=(r_2-r_3)/(r_1-r_3)$, $\alpha_2=(r_2-r_3)/(r_2-r_4)$, $g_1=\sqrt{4/(r_1-r_3)(r_2-r_4)}$, and χ_{10} and χ_{20} satisfy $r_1+(r_1-r_2)/(1-\alpha_1^2\text{sn}^2(\chi_{10},k_1))=0$, and $r_4+(r_3-r_4)/(1-\alpha_2^2\text{sn}^2(\chi_{20},k_1))=0$, respectively.

Choosing some special parameters c,g,h in (33) and (34), we can obtain breaking loop solutions [graphs are shown in Fig. 9 (9–1)–(9–5), also see Ref. 16).

VII. DYNAMICS OF THE LEVEL CURVES AND PARAMETRIC REPRESENTATIONS OF SOLUTIONS FOR SYSTEM (3′) WITH $n=\frac{1}{2}$

Finally, we consider dynamics of the level curves in Fig. 3 (3–1)–(3–6), which are determined by $H_{-1/2}(\phi,y)=h$.

For each given real number h, along the level curves, we have $y^2=\phi(h+16g\sqrt{\phi}+4\phi-\frac{16}{3}c\phi\sqrt{\phi})$. Taking integral on both sides of the equation yields

$$\int_{\phi_0}^{\phi}\frac{d\phi}{\sqrt{\phi\left(h-16g\sqrt{\phi}+4\phi-\frac{16}{3}c\phi\sqrt{\phi}\right)}}=\int_{\phi_0^2}^{\psi^2}\frac{\sqrt{3}d\psi}{2\sqrt{\frac{3}{16}h+3g\psi+\frac{3}{4}\psi^2-c\psi^3}}=\xi, \tag{35}$$

where ϕ_0 is an initial value.

Suppose $c>0$, $g>0$ [see Fig. 3 (3–1)], then in this case, $h_2<0$ and we have the following results.

When $h\in(h_2,0)$, the level curves $H_{-1/2}(\phi,y)=h$ take on a family of closed orbits that enclose the equilibrium point $E_2(\phi_2,0)$. In this case, we may get a family of periodic smooth wave solutions of (1) with $k=-\frac{1}{2}$ with the following parametric representation:

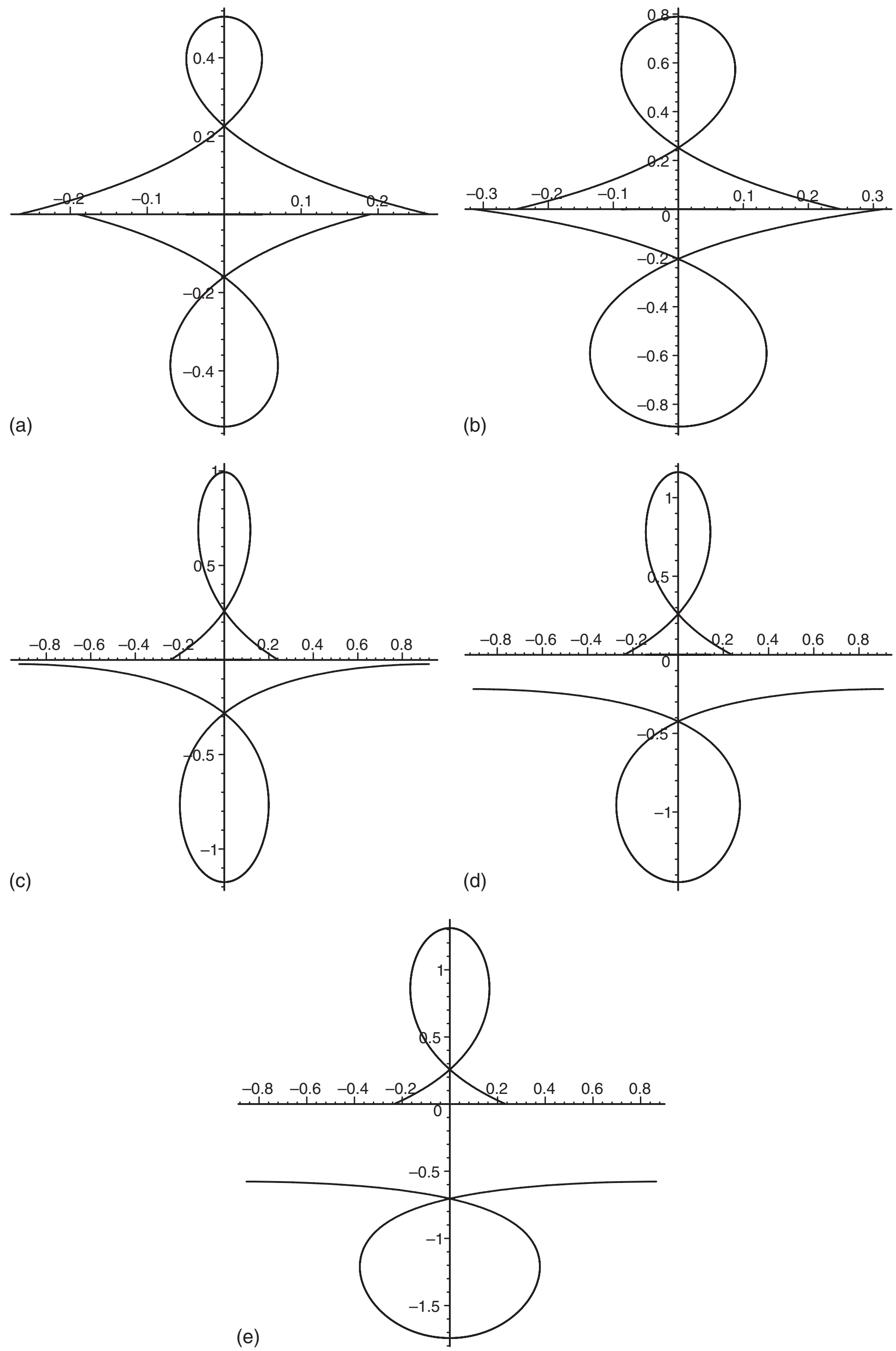

FIG. 9. The profiles of breaking loop solutions of two families of (1) with $k=-2$. Parameters: $c=1$, $g=-5$, $h_1=11.344\,751\,54$, $h_2=59.988\,581\,85$. (9–1) $h=h_1-10$. (9–2) $h=h_1-8$. (9–3) $h=h_1-6$. (9–4) $h=h_1-4$. (9–5) $h=h_1-2$.

$$\phi(\xi)=[\psi_a-(\psi_a-\psi_b)\mathrm{sn}^2(\omega_1\xi,k_1)]^2, \tag{36}$$

where $k_1=\sqrt{(\psi_a-\psi_b)/(\psi_a-\psi_c)}$, $\omega_1=\sqrt{\frac{c(\psi_a-\psi_c)}{3}}$, $\frac{3h}{16c}+\left(\frac{3g}{c}\right)\psi+\left(\frac{3}{4c}\right)\psi^2-\psi^3=(\psi_a-\psi)(\psi-\psi_b)(\psi-\psi_c)$, and $\psi_c<0<\psi_b<\psi_a$.

When $h=0$, the orbit determined by $H_{-1/2}(\phi,y)=0$ is still closed, and there is a periodic wave solutions of (1) with $k=-\frac{1}{2}$ with the following parametric representation:

$$\phi(\xi)=[\psi_a \mathrm{cn}^2(\omega_1\xi,k_1)]^2, \tag{37}$$

where $k_1=\sqrt{\psi_a/(\psi_a-\psi_c)}$ and $3h/16c+(3g/c)\psi+(3/4c)\psi^2-\psi^3=(\psi_a-\psi)\psi(\psi-\psi_c)$.

Remark: In the case of $h>0$, we have $\lim_{\phi\to 0} dy/d\phi = \lim_{\phi\to 0} 2\sqrt{h+16g\sqrt{\phi}+4\phi-(16/3)c\phi^{3/2}}/\sqrt{\phi}=\infty$, which implies that the y-axis is the tangent line of all closed orbits determined by $H_{-1/2}(\phi,y)=h$ $(h>0)$ at the origin $O(0,0)$. By the theory of singular traveling wave systems developed in Refs. 6, 7, and 14, we know that these closed orbits lead to infinitely many periodic wave solutions of (1) with $k=-\frac{1}{2}$, which have the same parametric representation as (36) with $\psi_c<\psi_b<0<\psi_a$, $\xi\in(0,\xi_M)$, and $\xi_M=(1/\omega_1)\mathrm{sn}^{-1}(\sqrt{\psi_a/(\psi_a-\psi_b)},k_1)$.

Suppose $c>0$, $-1/16c<g<0$. The graph of orbits are shown in Fig. 3 (3–2), and h_2, h_1 satisfy $0<h_2<h_1$.

When $h\in(h_2,h_1)$, the level curves determined by $H_{-1/2}(\phi,y)=h$ are a family of closed orbits, which enclose the equilibrium point $E_2(\phi_2,0)$. In this case, we also get a family of periodic wave solutions of (1) with $k=-\frac{1}{2}$, which have the same parametric representations as (36) with $0<\psi_c<\sqrt{\phi_1}<\psi_b<\sqrt{\phi_2}<\psi_a$. In particular, the family of closed orbits, tangent to the y-axis at the origin $O(0,0)$, generates the parametric representations of periodic wave solutions of (1) with $k=-\frac{1}{2}$ as follows:

$$\phi(\xi)=\left[\psi_b-\frac{(\psi_b-\psi_c)}{\mathrm{cn}^2(\omega_1\xi,k_1)}\right]^2, \quad \xi\in\left(0,\frac{1}{\omega_1}\mathrm{cn}^{-1}\left(\sqrt{\frac{\psi_b-\psi_c}{\psi_b}},k_1\right)\right), \tag{38}$$

where $k_1=\sqrt{(\psi_a-\psi_b)/(\psi_a-\psi_c)}$, $\omega_1=\sqrt{c(\psi_a-\psi_c)/3}$, and $3h/16c+(3g/c)\psi+(3/4c)\psi^2-\psi^3=(\psi_a-\psi)(\psi_b-\psi)(\psi_c-\psi)$.

When $h=h_1$, the level curves consist of one homoclinic orbit passing through the equilibrium point $E_1(\phi_1,0)$ and two heteroclinic orbits connecting the origin $O(0,0)$ to E_1. Accordingly, we can get a solitary, a breaking kink, and a breaking antikink wave solutions of (1) with $k=-\frac{1}{2}$. The solitary wave solution has the following parametric representation:

$$\phi(\xi)=[\sqrt{\phi_1}+(\sqrt{\phi_M}-\sqrt{\phi_1})\mathrm{sech}^2(\omega_0\xi)]^2, \tag{39}$$

where $\omega_0=\sqrt{c(\sqrt{\phi_M}-\sqrt{\phi_1})}/\sqrt{3}$ and $3h/16c+(3g/c)\psi+(3/4c)\psi^2-\psi^3=(\psi-\sqrt{\phi_1})\sqrt{\sqrt{\phi_M}-\psi}$. The breaking kink and antikink wave solutions have the following parametric representation:

$$\phi(\xi)=[\sqrt{\phi_1}-(\sqrt{\phi_M}-\sqrt{\phi_1})\mathrm{csch}^2(\omega_0\xi+\xi_0)]^2, \tag{40}$$

for $\xi\in(\mathrm{csch}^{-1}\sqrt{\sqrt{\phi_1}/(\sqrt{\phi_m}-\sqrt{\phi_1})},\infty)$ and $(-\infty,\mathrm{csch}^{-1}\sqrt{\sqrt{\phi_1}/(\sqrt{\phi_m}-\sqrt{\phi_1})})$, respectively, where $0<\phi_0<\phi_1$, $\xi_0=\mathrm{ctnh}^{-1}\sqrt{(\sqrt{\phi_m}-\sqrt{\phi_0})/(\sqrt{\phi_m}-\sqrt{\phi_1})}$.

When $h\in(h_1,\infty)$, the family of closed orbits, determined by $H_{-1/2}(\phi,y)=h$, are tangent to the y-axis at the origin $O(0,0)$ as well as enclosing two equilibrium points E_1 and E_2. In this case, we can get a family of periodic wave solutions of (1) with $k=-\frac{1}{2}$ with the following parametric representation:

$$\phi(\xi)=\left[A+\sqrt{\phi_a}-\frac{2A}{1+\mathrm{cn}(\omega_2\xi,k_2)}\right]^2, \quad \xi\in\left(0,\frac{1}{\omega_2}\mathrm{cn}^{-1}\left(\frac{A-\sqrt{\phi_a}}{A+\sqrt{\phi_a}},k_2\right)\right), \tag{41}$$

where $3h/16c+(3g/c)\psi+(3/4c)\psi^2-\psi^3=(\sqrt{\phi_a}-\psi)[(\psi+b_1)^2+a_1^2]$, $A^2=(b_1-\sqrt{\phi_a})+a_1^2$, $k_2^2=(A-b_1+\sqrt{\phi_a})/2A$, and $\omega_2=2c\sqrt{A/3}$.

When $h\in(0,h_2)$, the family of closed orbits determined by $H_{-1/2}(\phi,y)=h$ are tangent to the y-axis at the origin $O(0,0)$. In this case, we can also get a family of periodic wave solutions of (1) with $k=-\frac{1}{2}$ whose parametric representation is the same as (41).

Suppose $c>0$, $g=-1/16c$, then $\phi_1=\phi_2=1/16c^2$, $h_1=h_2=1/12c^2$. The graph of the corresponding orbits is shown in Fig. 3 (3–3).

When $h=1/12c^2$, there are two heteroclinic orbits that connect the origin $O(0,0)$ to E_1 and (E_2), respectively. In this case, we obtain a breaking kink and a breaking antikink wave solutions of (1) with $k=-\frac{1}{2}$, which have the following parametric representations:

$$\phi(\xi)=\left[\frac{1}{4c}-\frac{3}{c^2(\xi-\xi_0)^2}\right]^2 \quad \text{for} \quad \xi\in\left(\xi_0+\sqrt{\frac{12}{c}},\infty\right) \quad \text{and} \quad \left(-\infty,\xi_0+\sqrt{\frac{12}{c}}\right), \text{ respectively.} \tag{42}$$

When $h\in(1/12c^2,\infty)$ and $h\in(0,1/12c^2)$, the two families of closed orbits determined by $H_{-1/2}(\phi,y)=h$ are tangent to the y-axis at the origin $O(0,0)$. In this case, we get infinitely many periodic smooth wave solutions of (1) with $k=-\frac{1}{2}$, whose parametric representations are the same as (41).

Suppose $c>0$, $g<-1/16c$, the graph of phase orbits is shown in Fig. 3 (3–4). In this case, there is no positive equilibrium point of (13).

For each number $h\in(0,\infty)$, the family of closed orbits, determined by $H_{-1/2}(\phi,y)=h$, are tangent to the y-axis at the origin $O(0,0)$. In this case, we get a family of periodic wave solutions of (1) with $k=-\frac{1}{2}$, whose parametric representations are the same as (41).

Suppose $c<0$, $g<0$, then $h_1>0$ and the graph of phase orbits is shown in Fig. 3 (3–5). In this case, there exists only one equilibrium point $E_1(\phi_1,0)$.

When $h=h_1$, there are two heteroclinic orbits connecting the origin $O(0,0)$ to E_1. In this case, we obtain a breaking kink and a breaking antikink wave solutions of (1) with $k=-\frac{1}{2}$, which have the following parametric representations:

$$\phi(\xi)=[\psi_c+(\sqrt{\phi_1}+\psi_c)\tanh^2(\omega_3\xi+\xi_0)]^2, \tag{43}$$

for $\xi\in((1/\omega_3)\text{arctanh}\sqrt{|\psi_c|/(\sqrt{\phi_1}-\psi_c)}-\xi_0,\infty)$ and $\xi\in(-\infty,(1/\omega_3)\text{arctanh}\sqrt{|\psi_c|/(\sqrt{\phi_1}-\psi_c)}-\xi_0)$, respectively, where $\omega_3=\sqrt{c(\sqrt{\phi_1}-\psi_c)/3}$, $\xi_0=\text{arctanh}\sqrt{(\sqrt{\phi_0}-\psi_c)/(\sqrt{\phi_1}-\psi_c)}$, $3h/16c+(3g/c)\psi+(3/4c)\psi^2-\psi^3=(\sqrt{\phi_1}-\psi)^2(\psi-\psi_c)$, and $\psi_c<0<\sqrt{\phi_0}<\sqrt{\phi_1}$.

When $h\in(0,h_1)$, the family of closed orbits, determined by $H_{-1/2}(\phi,y)=h$, are tangent to the y-axis at the origin $O(0,0)$. In this case, we obtain a family of periodic wave solutions of (1) with $k=-\frac{1}{2}$, which have the following parametric representation:

$$\phi(\xi)=\left[\frac{\psi_b-k_3^2\psi_a\text{sn}^2(\omega_4\xi,k_3)}{\text{dn}^2(\omega_4\xi,k_3)}\right]^2, \quad \xi\in\left(0,\frac{1}{\omega_4}\text{sn}^{-1}\left(\sqrt{\frac{\psi_b}{k_3^2\psi_a}},k_3\right)\right), \tag{44}$$

where $\omega_4=c\sqrt{(\psi_a-\psi_c)/3}$, $k_3^2=(\psi_b-\psi_c)/(\psi_a-\psi_c)$, $3h/16c+(3g/c)\psi+(3/4c)\psi^2-\psi^3=(\psi_a-\psi)(\psi_b-\psi)(\psi-\psi_c)$, and $\psi_c<0<\psi_b<\sqrt{\phi_1}<\psi_a$.

VIII. CONCLUSIONS

In this paper, by using the method of planar dynamical systems and the theory of the singular traveling wave systems developed by the authors in Refs. 6, 7, and 14, we have discussed dynamical behavior for all possible traveling wave solutions of Eq. (1) for the cases of $k=-\frac{1}{2}$, $-2,\frac{1}{2},2$.

The main results are concluded as follows.

(i) For Eq. (1) with $k=-\frac{1}{2},\frac{1}{2},2$, all classical traveling wave solutions are smooth. In different (c,g)-parameter regions, we obtain all possible parametric representations of the bounded classical traveling wave solutions $\phi(\xi)$ of (1), including infinitely many smooth solitary wave solutions, periodic wave solutions, as well as kink and antikink wave solutions.

(ii) The most interesting case is $k=-2$ in Eq. (1). Because there exist two equilibrium points $S_{\pm}(0,Y_{\pm})$ of (11) on the straight line $\phi=0$, Eq. (1) with $k=-2$ has a cusp solitary wave solutions (peakon), and breaking loop solutions according to the theory developed in Refs. 6, 7, and 14. The parametric representations of these solutions have been provided.

To sum up, we give 25 parametric representations of the traveling wave solutions of (1) for $k=\pm 2, \pm \frac{1}{2}$. For all other k's, the dynamical behavior of traveling wave solutions can similarly be discussed by using the traveling systems (3) and their first integrals (4).

ACKNOWLEDGMENTS

J.L. is supported by the National Natural Science Foundation of China (Grant Nos. 10671179 and 10831003), and Z.Q. is partially supported by the U. S. Army Research Office under Contract/Grant No. W911NF-08-1-0511.

[1] M. J. Ablowitz and P. A. Clarkson, *Solitons, Nonlinear Evolution Equations and Inverse Scattering* (Cambridge University Press, Cambridge, 1991).
[2] M. Wadati, J. Phys. Soc. Jpn. **34**, 1289 (1973).
[3] M. Wadati, H. Sanuki, and H. Konno, Prog. Theor. Phys. **53**, 419 (1975).
[4] V. B. Matveev and M. A. Salle, *Darboux Transformation and Soliton* (Springer, Berlin, 1991).
[5] R. Hirota, Phys. Rev. Lett. **27**, 1192 (1971).
[6] J. B. Li and H. H. Dai, *On the Study of Singular Nonlinear Traveling Wave Equations: Dynamical System Approach* (Science, Beijing, 2007).
[7] J. B. Li and G. R. Chen, Int. J. Bifurcation Chaos Appl. Sci. Eng. **17**, 4049 (2007).
[8] Z. J. Qiao, J. Math. Phys. **48**, 082701 (2007).
[9] Z. J. Qiao and L. P. Liu, Chaos, Solitons Fractals **41**, 587 (2009).
[10] M. S. Alber, R. Camassa, Y. N. Fedorov, D. D. Holm, and J. E. Marsden, Commun. Math. Phys. **221**, 197 (2001).
[11] Z. J. Qiao, Commun. Math. Phys. **239**, 309 (2003).
[12] M. Kruskal, Lect. Notes Phys. **38**, 310C354 (1975).
[13] M. J. Ablowitz and H. Segur, *Soliton and the Inverse Scattering Transform* (SIAM, Philadelphia, 1981).
[14] J. B. Li, J. H. Wu, and H. P. Zhu, Int. J. Bifurcation Chaos Appl. Sci. Eng. **16**, 2235 (2006).
[15] P. F. Byrd and M. D. Fridman, *Handbook of Elliptic Integrals for Engineers and Sciensists* (Springer, Berlin, 1971).
[16] J. B. Li, Y. Zhang, and G. R. Chen, Int. J. Bifurcation Chaos Appl. Sci. Eng. **19**, 2249 (2009).